Iron atomic packing in Fe-Ru superlattices by x-ray-absorption spectroscopy

F. Baudelet, A. Fontaine, G. Tourillon, and D. Guay
Laboratoire pour l'Utilisation du Rayonnement Electromagnétique, Université de Paris–Sud, Bâtiment 209D, 91405 Orsay CEDEX, France

M. Maurer, M. Piecuch, M. F. Ravet, and V. Dupuis
Laboratoire Mixte, Saint-Gobain 54704, Pont-à-Mousson, France
(Received 6 February 1992; revised manuscript received 3 August 1992)

Unusual iron packing in Fe_xRu_y superlattices with x varying from 4 to 14 Å and y from 4 to 78 Å was observed by extended x-ray-absorption fine structure and x-ray-absorption near-edge-structure (XANES) analysis. The XANES profile and the first peak of the Fourier transform of the spectrum show a large anisotropy when the polarization of the x-ray synchrotron-emitted beam is in the basal plane of the superlattices or perpendicular to it. The local nature of this result suggests refinement of the structure already deduced by reflection high-energy electron diffraction and x-ray diffraction. The hexagonal packing of iron herein proposed agrees with the structural data found in the literature.

I. INTRODUCTION

Molecular-beam epitaxy offers the possibility of synthesizing layers and superlattices with sharp interfaces and well-controlled thicknesses. Of special interest are transition-metal films with modified structures because of the expected effects on magnetic properties due to variations of interatomic distances and crystal symmetry. It is, therefore, essential to have a correct knowledge of the local environment of the transition-metal atoms in these unusual phases.

The aim of the present work was to study the iron layers with a crushed hexagonal structure stabilized by epitaxial growth on the ruthenium buffer which is hcp. The iron hexagonal stacking shown by reflection high-energy electron diffraction (RHEED) and x-ray diffraction[1] has a ratio of approximately 1.55 and an atomic volume per Fe atom estimated to be 12.8 Å^3, surprisingly large compared to the usual bcc packing volume of 11.3 Å^3. The hexagonal iron phase exists above a pressure of 135 kbar under a volume per atom reduced to 10.9 Å^3. One of the most straightforward tools to study the local environment is x-ray-absorption spectroscopy (XAS), namely, extended x-ray-absorption fine structure (EXAFS) and x-ray-absorption near-edge structure (XANES), which give information selectively on the local geometry, and the nature and distance of neighbors around each atomic species.

Fe thin layers are known to be sensitive to the anisotropy generated by the interface. The Nd/Fe and Tb/Fe multilayers have an easy axis of magnetization perpendicular to the films for very thin layers (8 Å). The magnetization rotates to the in-plane direction for large thicknesses (30 Å in Tb/Fe) or high temperatures (200 K in Nd/Fe).[2]

It was expected that the hexagonal iron should exhibit such a behavior even with an enhancement of the magnetic moment, as found for Co layers sandwiched between gold or platinum.[3] The hexagonal packing is possible if imposed by the epitaxy on a ruthenium buffer. However, the observed magnetic properties of Fe/Ru are quite striking. Not only are the iron moments aligned parallel to the layers but Mössbauer spectroscopy shows a very surprising two-plane-thick magnetically dead layer.[4] In other words, magnetic moments appear only if the hexagonal iron layer is thicker than four (0001) planes. For thinner layers there is no local hyperfine field on iron atoms. It is not a mere disappearance of macroscopic moments due to antiferromagnetic ordering or a spin glass. This is a striking local property of this superlattice. Additionally, for thick layers the hyperfine field remains close to that found in the pure α iron structure. A recent theoretical study of the onset of magnetism in these superlattices gives a moment of the Fe atoms, assumed to be stacked in perfect hcp positions, of $2.6\mu_B$ for the middle iron layers with iron thicknesses greater than four atomic planes, instead of $2.1\mu_B$ found experimentally.[5]

Superlattices with various thicknesses of Fe and Ru were studied in order to investigate the nature of the stacking and the roughness of the interface versus both the thicknesses of Fe (4–14 Å) and Ru (4–78 Å). XAS takes advantage of the linear polarization of the beam emitted by a storage ring[6] to check the anisotropic character of the Fe neighborhood in this hexagonal structure. To stabilize these Fe/Ru superlattices, it is necessary to sandwich them between two thick ruthenium buffers that make any XAS investigation of the Ru environment useless.

XANES, which includes multiple scattering of the photoelectron by the neighbors, probes the local symmetry. It is now well documented that bcc metals such as V, Cr, and Fe have a characteristic bcc XANES spectrum, whereas Co hcp and Ni and Cu fcc show a XANES spectrum, very specific to close-packed stacking.[7,8] These fingerprints were recognized in the early days of XAS by Beeman and Friedman[7] and a recent illustration was given once again by Budnick *et al.*[9] to differentiate fcc Fe in Cu from bcc Fe in Cu 3 at. % Au solid solution. Very recent investigations at the Co K edge of Fe/Co multilayers that exhibit a Co bcc stacking consistent with NMR hyperfine fields show also a characteristic bcc XANES.[10]

On the other hand, investigation at the iron K edge in Ir/Fe superlattices where the iron is expected to be fcc shows a XANES profile characteristic of fcc (hcp) stacking with both orientations of the polarization for iron thicknesses as small as 5 Å.[11]

The radial distribution derived from the analysis of the EXAFS signal at the Co K edge confirms unambiguously the bcc type of cobalt in Fe/Co multilayers. All these data prove the ability of XANES to determine whether the local environment is bcc or hcp (fcc).

Surprisingly, XANES spectra of the Ru/Fe superlattices revealed a well-defined anisotropy of the Fe environment: the in-plane spectrum carries the hcp-like signature, whereas the out-of-plane spectrum is typical of a bcc-like packing. These experimental data address the question concerning the true nature of the iron hexagonal stacking, i.e., its departure from the ideal hcp model. Therefore, the packing proposed in this paper refines the stacking of the (0001) planes, taking into account the boundary conditions ($c=4.17$ Å) given by x-ray diffraction. Additional x-ray-diffraction data from in-plane reflections, undertaken to check the proposed model, confirm the difference between the "true" hcp packing and the present Fe hexagonal packing found in these superlattices.[12]

II. GROWTH OF SUPERLATTICES

The superlattices Fe_xRu_y were grown by UHV sequential deposition in a molecular-beam-epitaxy chamber (Riber EVA 32R&D) at pressures below 10^{-2} torr with two electron guns monitored by quartz balances. A 200-Å-thick buffer of Ru was sufficient to present any oxygen interdiffusion from the substrate $(11\bar{2}0)$ or $(1\bar{1}02)$ sapphire. The growth of the Fe hexagonal layer onto the (0001) plane of Ru shows an orientation that depends on the Miller index of the substrate: the c axis of Fe is perpendicular to the substrate in the $(11\bar{2}0)$ case and inclined by about 30° in the $(1\bar{1}02)$ case. This last point is of great importance regarding the ability to perform polarization-dependent x-ray absorption. The growth of superlattices has been investigated *in situ* by RHEED and Auger electron spectroscopy. No departure from a sixfold symmetry is detected for Fe thicknesses up to 14 Å from RHEED. An enlarging of the streak is probably due to strains within the Fe layer, but a coverage of two layers of Ru is sufficient to eliminate this broadening, i.e., to eliminate most of the defects of the Fe layer.

X-ray scattering with the diffraction vector along the growth axis in the $(11\bar{2}0)$ sapphire case (c) proves the good quality of the epitaxy and the periodicity of the stacking.[13] The stacking sequence is found to be $ABAB$,[1] as with an hcp packing and not the $ABCABC$ of the fcc one. Because of the two-dimensional character of the sample, it is more difficult to get information about the iron environment in the basal plane with x-ray diffraction. Diffraction gives an average description of the crystal, i.e., the virtual crystal. It is therefore necessary to measure the local distances to refine the picture of the real crystal built by Fe and Ru crystalline layers. Local probes such as EXAFS and XANES are therefore appropriate.

III. POLARIZATION-DEPENDENT XAS

X-ray-absorption spectroscopy measurements have been performed at the Laboratoire pour l'Utilisation du Rayonnement Electromagnétique, using the x-ray beam delivered by the DCI storage ring, which is operated at 1.82 GeV with beam intensities typically larger than 250 mA and a lifetime better than 50 h. Absorption spectra have been measured at the Fe K edge (7112 eV) using a channelcut Si 331 monochromator. Fe K edge EXAFS experiments have been carried out on Fe_xRu_y superlattices with x varying from 4 to 14 Å and y ranging from 4 to 78 Å on a $(11\bar{2}0)$ sapphire substrate, with the growth axis along the c axis of Fe and Ru.

The presence of a thick substrate prevents one from

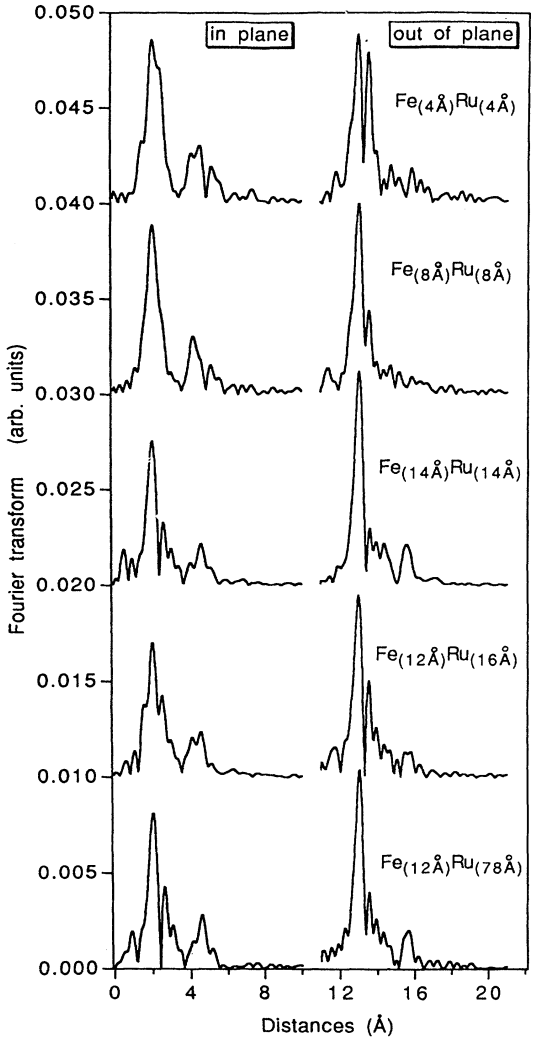

FIG. 1. Two sets of Fourier transforms of the spectra of superlattices with various thicknesses of iron and ruthenium in both orientations of the incident-light electric field: in-plane on the left-hand side and perpendicular on the right-hand side. The splitting of the main peak is due to interferences between the iron and ruthenium contributions in the perpendicular $Fe_{4\,Å}Ru_{4\,Å}$ case, or mainly to the two Fe-Fe distances for the thick iron layer in both polarization directions.

collecting data using the classical transmission mode. It is necessary to use a decay process such as fluorescence for a dilute sample or electron yield for a concentrated sample.[14] The intensity of the decay channel is proportional to the probability of creating the core hole by the photoelectric effect.[15] The energetic photoelectron Auger emitted from an x-ray-illuminated sample are converted to a cascade of low-energy electrons in the sample or in the He atmosphere of the sample chamber. The signal is collected on a biased electrode and the x-ray-absorption spectrum is recorded by scanning the energy of the incident photons step by step. Fluorescence-detection spectra have been carried out on very dilute samples, such as the solid solutions used as references to extract phase shifts and amplitudes of the Fe-Ru pair.

We took advantage of the polarization of the synchrotron beam, since the contribution of the neighboring atoms is angular dependent ($3\cos^2\theta$), where θ is the angle between the electric vector of the incident beam and the relative-position vector of the neighbors. In an ideal hcp stacking ($c/a=1.63$), the weight of the neighbors varies strongly with the direction of the electric field. In the basal plane, weights are 1.5, 9, and 1.5 for the upper, in-plane, lower atoms, respectively; perpendicular to it, we get 6, 0, and 6, respectively. These three values need to be compared with the real number of next neighbors, which are 3, 6, and 3 in a perfect hcp stacking.

The weights are distance dependent for the in-plane measurement as well as for the perpendicular case. The present iron stacking differs from the ideal hcp one but the structural differences induce only a small variation of these three weights. Nevertheless, the slight corrections are easy to incorporate into the fitting procedure. The EXAFS spectra show strong differences when the electric field is rotated from the in-plane polarization to the perpendicular polarization. Obviously, we need to keep a small glancing angle (typically 5°) in order to illuminate the sample with the incident beam. A regular EXAFS data analysis goes with the Fourier transform of the oscillations[16] of the spectra (Fig. 1). Part of the EXAFS spectra shown herein are beats in the momentum space which are viewed as split peaks in the pair-distribution function in the real space. The origin of the beat will be described later.

IV. ANALYSIS OF THE EXAFS SPECTRA

A. Theoretical aspects

The origin of the EXAFS signal is well established and has been discussed at length.[16] If multiple scattering effects are neglected, which is correct at least in the high-energy part of the spectrum, the EXAFS modulations are described in terms of interference between the outgoing and the backscattered photoelectron wave functions within the so-called plane-wave approximation, as follows:

$$\chi(k)=-\frac{1}{k}\sum_j \frac{1}{R_j^2}3\cos^2\theta_j \exp(-2\sigma_j^2k^2)\times\exp\left[\frac{-2R_j}{\lambda(k)}\right]|f_j(\pi,k)|\sin\Phi_j(k)\ ,$$

with

$$\Phi_j(k)=2kR_j+2\delta(k)+\arg[f_j(\pi,k)]\ .$$

Here, k is the photoelectron momentum, R_j the distance of the atom j from the excited atom, σ_j its Debye-Waller factor, and $\lambda(k)$ the mean free path of the photoelectron. The phase shift $\Phi(k)$ involves two components: the first ($2kR_j$) is the optical path to the neighbors j, and the other terms come from the phase lag due to the travel through the potentials of the absorbing and backscattering atoms, δ and arg $[f_j(\pi,k)]$, respectively. $f_j(\pi,k)$ is the complex backscattering amplitude; both its modulus and its phase allow the chemical identification of the backscattering atom.

B. Standard sample for phase-shift and amplitude determination

Structural results require a good knowledge of these parameters. The best procedure is to use as references well-known compounds or alloys whose structures are closely related to system under investigations. In the present study, we need such parameters for Fe-Fe and Fe-Ru pairs. Phase shifts and amplitudes of the latter have been found from Ru 2 at. % Fe solid solution, which has a hexagonal structure. It is worthwhile to underline that with the same absorbing atom (iron), the phase shift of iron-ruthenium is out of phase (by about π) with respect to the iron-iron pair [Fig. 2(a)] for a k value of about 6 Å^{-1} derived from EXAFS. Deduced phase shifts and amplitudes have also been checked by analyzing the spectrum of the intermediate compound $RuFe_3$. Since at room temperature Fe is bcc, the first shell (eight neighbors at 2.48 Å) and the second shell (six neighbors at 2.86 Å) are unresolved in the Fourier transform, which means that one cannot directly determine phase shifts and amplitudes.[17] However, it is possible to get accurate values using an experimental determination of the Co-Co pair EXAFS parameters plus a small theoretical correction to account for the step down of the Z number. The Co foil was measured at room temperature and phase shift and amplitude were extracted. The theoretical corrections have been found in the McKale table. The correction is 5% for the amplitude and is negligible for the slope of the phase shift. These parameters lead to a perfect simulation of the partial EXAFS signal built with the first two shells of the bcc Fe.

Now we discuss two origins of the splitting of the first peak of the radial distribution. The Fourier transform of the EXAFS spectrum of the superlattice $Fe_{4\ Å}Ru_{4\ Å}$ measured with the in-plane polarization shows a single main peak. This peak is split when the polarization is close to the c axis (Fig. 1). This splitting in the real space corresponds to a beat in the momentum space (Fig. 3). For the small values of k, the iron and ruthenium backscatterers have the same phase shift (modulo 2π) [Fig. 2(a)]. For k values larger than 6 Å^{-1} the Ru phase shift is out of phase by almost π compared to the Fe one. When the ruthenium contribution starts to dominate the iron contribution [Fig. 2(b)] the phase of the EXAFS modulation changes by π more or less, which leads to a beat. Simu-

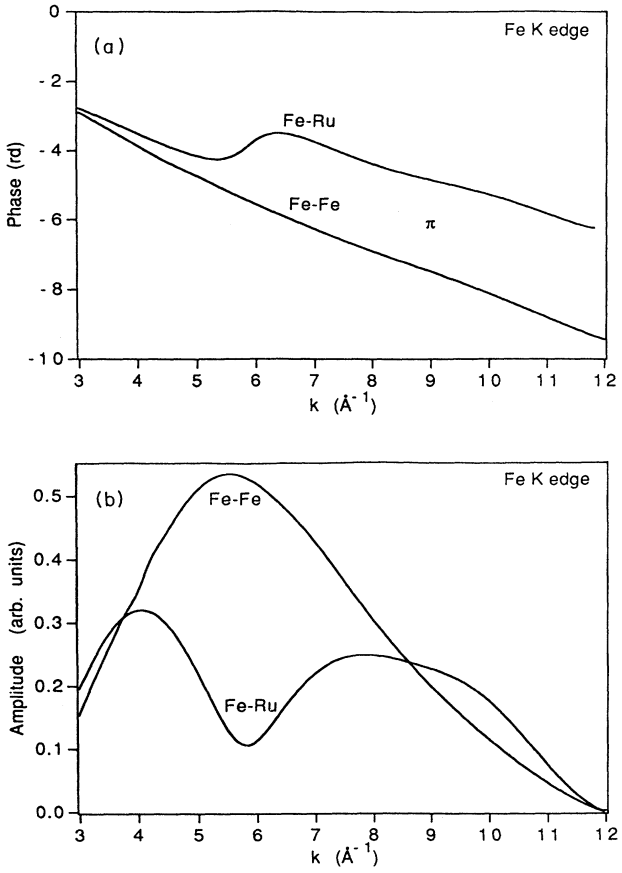

FIG. 2. Experimental Fe-Fe and Fe-Ru phase shifts and amplitudes extracted, respectively, from a pure Co metal foil with a slight theoretical correction, and from solid-solution Fe 2 at. % Ru well characterized by x-ray diffraction. A difference of about π between the two phase shifts in a large (k) domain (a) leads to a great sensitivity to the presence of Ru atoms in the neighborhood of the absorber atom.

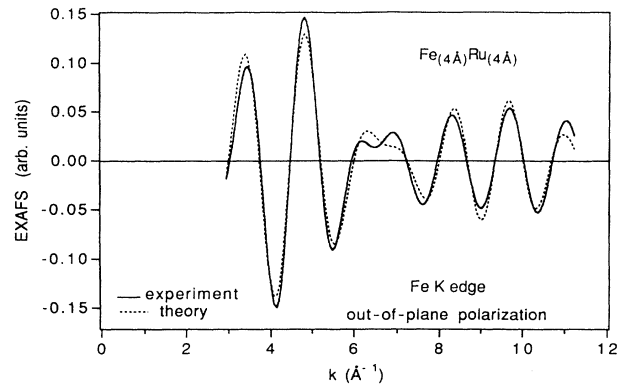

FIG. 3. Filtered EXAFS oscillations for the perpendicular $Fe_{4\ \text{Å}}Ru_{4\ \text{Å}}$ case. According to the phase shifts and amplitudes of Fig. 2, the contribution of iron neighbors dominates at low k and the contribution of ruthenium atoms dominates at high k. For an intermediate value of k (about 6 Å^{-1}) the phase of these oscillations changes by π, which generates a beat corresponding to a split peak in the real space.

lated Fourier transforms where Fe and Ru neighbors are mixed with various respective numbers keeping 12 as a total demonstrate very well this splitting effect. This situation has already been encountered for the Zn-Al and the Zn-Zn atomic pairs.[18]

The splitting of the Fourier transform (FT) of the in-plane spectra of superlattices with thick iron layers (Fig. 1) as $Fe_{12\ \text{Å}}Ru_{78\ \text{Å}}$ is also a manifestation of a beat in the momentum space but, conversely to the preceding case, the π difference comes from the optical path in $\Phi(k)$, i.e., $(2kR)$, when two shells of the same atomic nature exhibit a difference $\Delta R = R_i - R_j \sim 0.25$ Å; $(2k\Delta R)$ is close to π for k vaues about 6 Å^{-1}. Therefore, the FT splitting either reflects two distances of iron or reveals the presence of ruthenium.

V. RESULTS

With good phase shifts and amplitudes for each atom pair, the next step of the data analysis is to fit the EXAFS spectra of superlattices using the distances, the nature of neighbors, and the relative number as free parameters. Consistency must be found between in-plane and normal polarization data. For all spectra, a decomposition into two subshells of iron and sometimes a third shell of ruthenium is strongly suggested by the above discussion. Several superlattices with various thicknesses of iron and ruthenium have been proved by EXAFS and XANES (Fig. 4).

The energy scale is calibrated from a zero position aligned to the first maxima in the derivation spectra of pure iron. This zero value of the kinetic energy of the photoelectron is assigned to be the 7112 eV at the iron K edge. The preedge background removal uses a simple

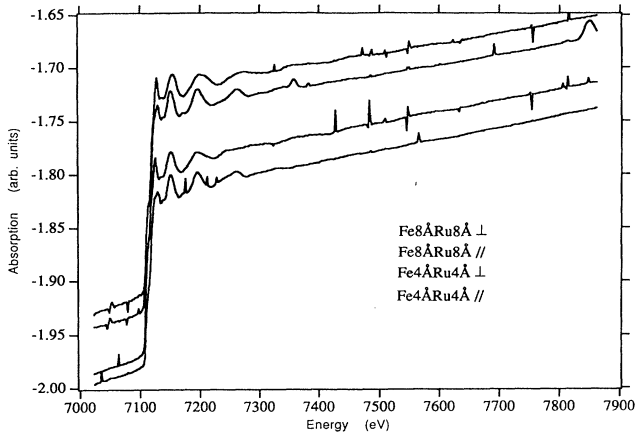

FIG. 4. Raw data of two superlattices and two orientations of the incident electric field. The glitches are mainly due to the very high crystallinity of the probed compound. For in-plane measurements, we can find a good incidence for avoiding most of the glitches. For the perpendicular measurements, we have to keep the grazing incidence, which leads to more glitches. Various measurements with small changes in incidences show that the results are not affected by the presence of these glitches.

three-order polynomial substraction. About 80 eV above the edge we take an inflection point in oscillation as a normalization point, the step height is made equal to 1, as it is the standard process for both the reference and the probed compounds. The normalized spectra of the fine-structure oscillations are reextracted using a spline code. The experimental fine-structure oscillations are Hanning windowed in the same conditions exactly, before Fourier transform. The filtered oscillations in **k** space are modeled using the $\chi(k)$ formula of Sec. IV A, using the experimental phases and amplitudes. The current free parameters are fitted in about 20 steps, using the usual least-square criterion which is taken as the quality factor. In a first step, we keep only the distances and the relative number of neighbors as free parameters. According to the standard criteria in XAFS,[19] the maximum number of free parameters to be used is about ten, since the number of independent data points $N_{\text{idp}}=2\Delta k\Delta R/\pi$, where Δk and ΔR are, respectively, the widths in **k** space (8 Å^{-1}) and R space (2 Å) used in the present data analysis. The total number of neighbors is fixed according the expected structure. The Debye-Waller factor and the mean free path are not allowed to vary because of the use of experimental phase shifts and amplitudes, which means that disorder is expected to be roughly the same in the probed superlattices and in the reference alloy. This gives eight free parameters in the three-shell fits and five in the two-shell fits. A good consistency must be found between the two sets of outputs from the in-plane and out-of-plane data. It provides an extra condition of validity that constrains the fitting procedure drastically following the international standard criteria. In a second step, when a good agreement with the fit of both polarization data is found, i.e., the same distances and consistent number of neighbors for each shell, we again start a fit with the Debye-Waller factor as a free parameter. Obviously, what is found is a change in the Debye-Waller factor. A negative value means that the probed bond is more "ordered" than the reference compound.

Experimentally, the plane-wave formalism, in conjunction with the phase shifts and amplitudes extracted by referencing to interatomic distances comparable to the distances found in the superlattices, contain the spherical-wave-induced correction. The error bar of the adjusted parameter comes from statistics over fitting of EXAFS oscillation extracted from spectra of well-characterized Fe_xRu_{1-x} alloys with x varying from 0 to 1, with a 0.1 step.

For almost all superlattices with the c axis perpendicular to the plane (Table I), the in-plane spectra give about nine effective in-plane Fe neighbors located at (2.73 Å). These nine effective neighbors can be converted to six real neighbors if we keep in mind a hexagonal packing regardless of what the unit cell is. The out-of-plane Fe distance is much shorter (2.50 Å) than the in-plane one for practically all multilayers. This distance is a little larger in two cases, $Fe_{4\text{ Å}}Ru_{4\text{ Å}}$ and $Fe_{8\text{ Å}}Ru_{8\text{ Å}}$ (2.56 and 2.54 Å, respectively). The out-of-plane effective coordination number, given by $\sum_i 3\cos^2\theta_i$, can be converted to a real count of neighbors, but this last value is model dependent. This point will be clarified later on. On thicker superlattices, Table I shows the general agreement through the whole set of measurements, which include polarization-dependent spectra.

Therefore, two Fe-Fe distances are deduced: one for in-plane neighbors (2.73±0.03 Å) and one for out-of-plane neighbors (2.50±0.02 Å). These two distances come from two independent analyses of the in-plane and out-of-plane spectra that contain weighted contributions of these two sets of iron distances. There is a remarkable consistency between the two independent EXAFS evaluations of these distances. Let us point out that, because of the change of their relative weights in each spectra, the in-plane distances (2.73 Å) are better seen with the polarization put in plane and the out-of-plane distance (2.50 Å) with the out-of-plane polarized data.

Regarding the nature of the nearest neighbor with respect to the Fe absorber, the number of Ru atoms in plane is always negligible, except possibly in the $Fe_{4\text{ Å}}Ru_{4\text{ Å}}$ case, where a maximum of 10% substitution is detected. This is an additional proof that intermixing

TABLE I. In-plane and out-of-plane distances with effective coordination numbers measured by the two sets of experiments (polarization in plane and out of plane). Here, N_1 number of in-plane Fe neighbors, N_2 number of out-of-plane Fe neighbors, D_1 and D_2 are their distances, respectively, $\Delta\sigma_1$ and $\Delta\sigma_2$ are relative to the reference Debye-Waller factor, and N_3,D_3, and $\Delta\sigma_3$ apply to the Ru neighbors. (Their values are shown in parentheses.) The c axis is perpendicular to the substrate.

		In-plane polarization (∥)						Out-of-plane polarization (⊥)					
x		N_1	D_1	N_2	D_2	$\Delta\sigma_1$	$\Delta\sigma_2$	N_1	D_1	N_2	D_2	$\Delta\sigma_1$	$\Delta\sigma_2$
	y	N_3	D_3			$\Delta\sigma_3$		N_3	D_3			$\Delta\sigma_3$	
4		9	2.73	1.5	2.55	.001	−.003	0		6	2.56		.006
	4	(1.5)	(2.57)			(001)		(6)	(2.60)			(−.001)	
8		8.9	2.69	2.1	2.53	.015	0	0		9	2.54		.009
	8							(3)	(2.6)			(−.003)	
14		7.2	2.74	3.8	2.50	.011	−.002	0.5	2.8	7.7	2.49	−.009	.005
	14												
12		8.9	2.70	2	2.50	.018	−.003	4	2.715	4.4	2.47	.008	−.003
	16												
12		8.9	2.75	2	2.50	.018	−.003	5.1	2.78	5	2.49	.004	−.003
	78												

is negligible and that interfaces are of great quality, as suggested by diffraction data. The inclusion of the third shell of ruthenium is needed obviously when the iron thickness is small, typically 4 Å with the polarization in both directions.

The two Fe-Fe distances (in plane and out of plane) found in the superlattices give a crystallographic parameter c of 3.88 Å if we assume a classical $ABAB$ hexagonal compact stacking (12 next neighbors). This value for c is too small compared to the unambiguous value established by x-ray diffraction (4.15 Å) and a (a) value estimated to be 2.66 Å assuming a regular hexagonal packing. This model assigns neighbors to be located at 2.66 and 2.58 Å, respectively.

VI. DISCUSSION

To account for diffraction results, which give c and a only, and EXAFS ones, which give strictly next-neighbor positions, we need to propose a model of the structure that fits both the c value deduced by x-ray diffraction and the swelling of the hexagonal stacking derived from the local distances found by EXAFS. The only way to proceed is to translate one dense-plane (0001) plane with respect to the other. This leads to the nonclassical $AB'AB'$ stacking, where the B' atoms now sit on a bridging position just above the midpoint of a side of the triangle (Fig. 6) instead of the center of gravity. Each atom is then surrounded by 14 neighbors and this hexagonal packing gives a c value of 4.18 Å, which is close to the diffraction result.

As mentioned previously, the first evidence for this model comes from the XANES results. Besides EXAFS, which is only sensitive to pair distribution, the profile of absorption edges is a powerful probe sensitive to the symmetry of the atomic structure, since it is driven by multiple correlation functions beyond the mere pair one. Since XANES simulations are still out of reach for most groups, we use XANES as a fingerprint which is efficient in case of significant differences. A simple comparison of the Fe XANES in Fe/Ru superlattices is shown with the XANES of 3d metals: hexagonal close-packed Co (12 nearest neighbors) and bcc Fe (8+6 coordination) (Fig. 5). A striking observation is that when the polarization is in the basal plane, the Fe XANES is identical to the Co one as evidence of a hexagonal local structure, in good agreement with the RHEED pattern. When the polarization is perpendicular to the basal plane, XANES departs from a typical hcp fingerprint and shows similarities to a bcc-type XANES for iron thicknesses up to 14 Å. This result is consistent with the unusual hexagonal stacking proposed, which retains the good expitaxy of the iron (110) bcc-like layer on the ruthenium (0001) hcp plane.

A small deformation makes the (110) iron bcc-like plane hexagonal. This is the usual first step of the α-to-γ phase transition, namely the Martensitic transformation. In this case the γ-iron environment shows a sixfold symmetry in the basal plane. This is not realized in the present case, since two "hats" of four neighbors are generated above and below, applying the same deformation to the next 110 planes, which keep a 14-fold coordination

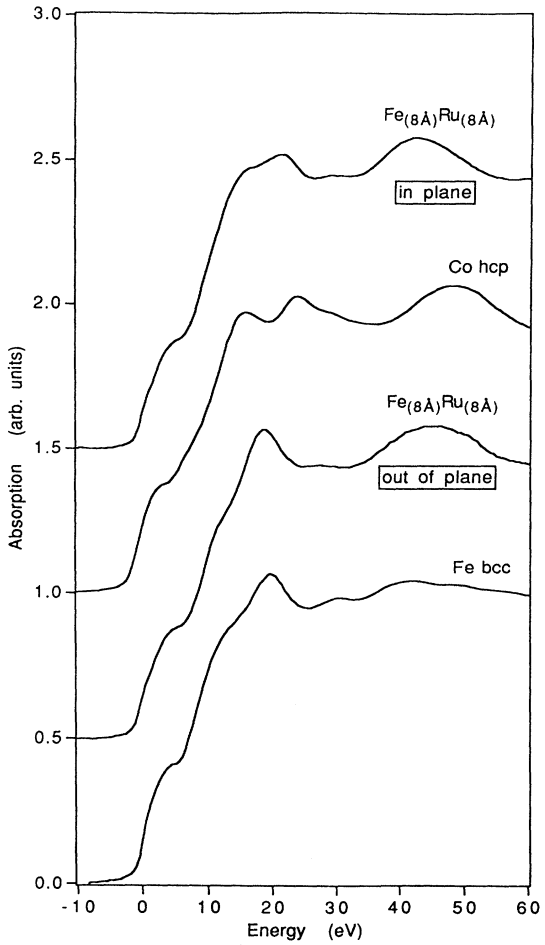

FIG. 5. Strong anisotropy of the XANES spectra is detected between the in-plane and out-of-plane polarization in all superlattices with the c axis perpendicular to the substrate and Fe thicknesses from 4 to 14 Å. The in-plane XANES is similar to an hcp-type XANES spectrum, such as that found for the cobalt metal. The out-of-plane XANES is of bcc-type, as found for iron metal.

(Fig. 6). Focusing our attention on the B plane of the $ABAB$ hcp packing, this structure comes from a mere translation toward the midpoint of the side of the triangle. The sixfold global symmetry of the hexagonal packing appears as an average between three possible translations that could generate domains of limited extension. This noncompact "hcp" structure can be discriminated from the hcp one only by a very careful x-ray-diffraction study of Bragg-peak intensities along $(10\bar{1}0)$ which have been performed by Raoux and DeSantis.[12] This investigation shows a departure from the pure regular hcp iron phase. Regarding the $10\bar{1}0$, $20\bar{2}0$, and $30\bar{3}0$ peaks, their respective theoretical intensities are 1,1,1 for an hcp when normalized by the structure factor and 1,12/7,4/7 for the proposed hp stacking. The corresponding experimental values are 1,1.7,0.57 which is a good fit to our model. These data tend to confirm our hp model and rule out the perfect hcp stacking.

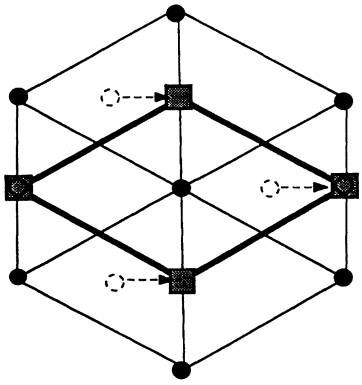

FIG. 6. The proposed hexagonal packing $AB'AB'$ deals with a shift of the B' plane from the center of the triangle (as it is in the hexagonal compact structure) to the middle of one side of the triangle. (One of the three possibilities is represented.)

We now investigate other possible models, since it is compulsory to keep the sixfold symmetry of the average structure, which is clearly shown by diffraction data. The only possibility is to again use analogous translations to shift B-type planes with respect to A, keeping the magnitude of such translations smaller than the proposed one $a2\sqrt{3}$. It leads to a rather poor local symmetry with the diamondlike hats of the upper and lower planes not being centered on the top of the A atoms. The B' position has the advantage of mimicking the bcc structure and being more symmetrical, and mainly gives a correct c value.

The effective in-plane number calculated with such a model is

$$9=\sum_{1}^{6} 3\cos\theta^2 ,$$

where the in-plane polarization and the effective out-of-plane number reaches 1.7 by keeping the four closer neighbors. The other four atoms, two at the top and two at the bottom, are much farther (3.17 Å) apart. The experimental values (9 and 2) are close to these two values except for the $Fe_{14\ Å}Ru_{14\ Å}$, which was known to exhibit a large roughness (about three atomic planes) as evidenced by diffraction.[20] To account for the larger Fe out-of-plane distances found for $Fe_{4\ Å}Ru_{4\ Å}$ or $Fe_{8\ Å}Ru_{8\ Å}$, one should look to the real hcp packing as an alternative possibility. The hcp packing gives c values that are too short, 4.03 and 3.98 Å, respectively, which is still far from the diffraction datum 4.15 Å. On the other hand, this datum is smaller than the two values 4.33 and 4.28 Å given by the hexagonal model proposed above. One should think of an intermediate situation where the two-plane-thick Fe layer, or, to a smaller extent, the four-plane-thick Fe layer, may be made of an admixture of the two hexagonal stackings. Given the c value expected, the hcp stacking accounts for roughly 50% and 25% for $Fe_{4\ Å}Ru_{4\ Å}$ and $Fe_{8\ Å}Ru_{8\ Å}$, respectively. Such a difference between the thinner layers and the others may be the source of the first two magnetically dead iron layers but it requires a nontrivial process which, at this point, is difficult to understand.[4]

The effective in-plane number calculated with the proposed hp model with the polarization set perpendicular gives an in-plane contribution equal to zero neighbors, but this value depends strongly on the real angle between the incident field polarization and the normal. We find an important in-plane contribution in the $Fe_{12\ Å}Ru_{16\ Å}$ and $Fe_{12\ Å}Ru_{78\ Å}$ cases, where a glancing angle was not smaller than 45° (instead of 5°) because of the small size of the sample. However, these sets of values remain very important in confirming the two distances deduced from the in-plane-polarization data.

The presence of the third distance of 3.17 Å gives a Fourier transform with an enlarged foot of the main peak. This high distance contribution is very difficult to isolate by any process. It leads to a small shift of the center of gravity of the peak. This is probably the reason why the Fe-Fe distance of 2.73 Å found by EXAFS is a little greater than the value of 2.71 Å expected from a perfect epitaxy of Fe on the Ru lattice.

Results on samples with a c axis inclined by about 30° with respect to the normal of the sample will be related elsewhere (epitaxy on sapphire). There is no simple way in this case to interpret the polarization dependence of the number of neighbors in each electric-field orientation. Again, the main result is the presence of two iron-iron distances similar to those found with the first set of superlattices.

The EXAFS analysis generates other useful informations about the iron stacking: The anisotropic result of the $Fe_{4\ Å}Ru_{4\ Å}$ proves the great quality of the interfaces with absolutely no interdiffusion between the iron and the ruthenium. Superlattices with 12-Å-thick iron and ruthenium thicknesses of 4, 12, and 20 Å show that ruthenium can impose the iron hp structure even if it is only 4 Å thick.

The iron retains the hp structure for thicknesses up to 14 Å. The Debye-Waller factor used in fitting the in-plane polarized EXAFS increases with the iron thickness, which is consistent with the presence of strain defects suggested by the enlarging of the RHEED streak.

Polarized XANES investigations of the Ru K edge confirms the hcp structure of ruthenium in both directions. However this is expected for the upper buffer of Ru and its only advantage lies in showing what kind of XANES fingerprint can be expected from a hcp structure when tilting the angle of the electric field with respect to the surface.

VII. RELATION BETWEEN MAGNETISM AND STRUCTURE

Besides the magnetic and crystallographic phases of bulk iron, new phases can be stabilized by epitaxy. They lead to a great diversity of magnetic properties, since "new materials" can be made with "old elements."[21]

The hexagonal solid solution Fe_xRu_{1-x}, where the lattice parameter changes from $a=2.706$ Å for $x=0$ and

$a = 2.75$ Å for $x = 0.75$, is not magnetic for all $x < 0.75$.[22] The Co/Ru superlattices, also hexagonal compact with a high structural perfection and rough interfaces, are magnetic and show an antiferromagnetic coupling between the Co layers.[23]

The Fe/Ru superlattices have very surprising properties that contradict common sense. The large increase of the interatomic iron distances should give larger magnetic moments because of the narrowing of the electronic bandwidth. Furthermore, when the exchange energy decreases, the order temperature decreases also. Nevertheless, we observe the following.

Two dead atomic layers, not magnetic, are found just near the interface. The layer is ferromagnetic only for thicknesses greater than those for atomic layers. The Mössbauer data at 4.2 K confirm the presence of two iron sites, which can be well explained if we consider that the magnetic atomic layers are in the core of the Fe layer, sandwiched by two dead atomic layers, and a moment of $2\mu_B$ per atom is found when the thickness is bigger than four atomic layer. The increase of interatomic distances does not increase the magnetic moment per iron atom. The intensity ratio of the six Mössbauer peaks gives an in-plane magnetization for thick Fe layers.

The sixfold axial symmetry is clearly confirmed by the angular dependence of the quadripolar doublet observed in the Mössbauer spectroscopy. Nevertheless, the intensity ratio is not the expected value for a hexagonal compact stacking: 0.48 instead of 0.33. The isometric shift is very similar to the bulk iron one: 336 kOe for the superlattice Fe/Ru, compared with 340 kOe for the bulk iron and 343 kOe for the iron thin film.

The Mössbauer spectroscopy confirms clearly the hexagonal stacking of the iron by epitaxy on the ruthenium, but suggests strongly that the regular hcp stacking is not achieved. On the contrary, the hp structure proposed above is found to be in good agreement with the magnetic results, consistent with the fact that the $AB'AB'$ stacking retains the large number of near neighbors of the bcc structure.[14]

Recent calculations by Knab and Koening[24] show that the hp stacking induces a ferromagnetic intralayer order as it is experimentally observed. On the contrary, the hcp stacking gives an antiferromagnetic order. Furthermore, the stability of the ferromagnetic order in the hp structure is greater than the antiferromagnetic order with the hcp structure (80 mRy instead of 50 mRy). Similarly, the hp ferromagnetic order is more stable by 30 mRy than the hp antiferromagnetic order.

These theoretical results are not surprising if we keep in mind that the hp structure is derived from the bcc one. It is well known that the stability of the bcc structure corresponds to a minimum in the density of state near the Fermi level. In the hp structure, the density of majority spin states remains quite small, which is not the case for the hcp structure.[5,24]

The last point of the discussion concerns the magnetic dead layers. The experimental data show that for thicknesses below 8 Å (four atomic layers) the hp stacking is not fully established. The presence of both types of stacking (hp and hcp) envisaged above could be at the origin of the presence of the dead layers, but the mechanism is not clear. Regarding the x-ray data, it is not possible to invoke a solid-solution effect due to intermixing.

VIII. CONCLUSION

EXAFS and XANES experiments take advantage of the linear polarization to probe anisotropic synthetic crystals. Differences in the real structure of iron with respect to the virtual lattice suggested by x-ray diffraction show that the iron layer does not have the classical hcp structure. However, it is a hexagonal packing but with an unusual stacking of the AB planes that can be seen as an epitaxy of the (110) bcc-like planes of iron on the 0001 hcp plane of ruthenium. These epitaxial conditions are compatible with the overall sixfold symmetry.

The c parameter of 4.18 Å is in good agreement with the x-ray-diffraction results. The atomic volume of iron of 12.8 $Å^3$ is large compared to the 11.3 $Å^3$ in the usual bcc packing. The coordination number is kept equal to 14, as it is with bcc. Such a structure can help to explain the bcc-like hyperfine field found by Mössbauer. The EXAFS analysis of the $Fe_{4\,Å}Ru_{4\,Å}$ confirms the great quality of the interfaces with essentially no interdiffusion between Fe and Ru.

Further extensive in-plane diffraction measurements should be carried out to check our model of the iron hexagonal packing. We expect significant results to come from multiple-scattering calculations to simulate XANES in both orientations of the sample with respect to the polarization.

The local out-of-plane expansion measured for the two thinner layers (4 and 8 Å), which is compatible with none of the $ABAB$ hcp stackings or the $AB'AB'$ present model, may be correlated with the lack of magnetism. As soon as the local bcc-like environment is established, the magnetic moment exhibits roughly the bcc hyperfine field. It is more an experimental correlation than a prediction, since the energies between the different stackings differ by a quantity of the order of 0.01 eV/atom. But we know that magnetism stabilizes the bcc structure of iron against the fcc one.

ACKNOWLEDGMENT

The Laboratoire pour l'utilisation du Rayonnement Électromagnétique is supported by CNRS, CEA, MENC, and the Laboratoire Mixte is "Unité Associée du Centre National de la Recherche Scientifique."

[1]M. Maurer, in *Growth, Characterization, and Properties of Ultrathin Magnetic Films and Multilayers,* edited by B. T. Jonker, J. P. Heremans, and E. E. Marinero, MRS Symposia Proceedings No. 151 (Materials Research Society, Pittsburgh, 1989), p. 99.

[2]F. Baudelet *et al.*, Phys. Rev. B **43**, 5857 (1991).

[3]Roy Clarke *et al.*, J. Magn. Magn. Mater. **93**, 53 (1991).

[4]J. P. Sanchez *et al.*, Hyperfine Interact. **57**, 2077 (1990).

[5]D. Knab and C. Koenig, Phys. Rev. B **43**, 8370 (1991).
[6]D. Laudy, Nucl. Instrum. Methods A **290**, 248 (1990).
[7]W. W. Beeman and H. Friedman, Phys. Rev. **56**, 392 (1939).
[8]J. Wong, Phys. Rev. B **30**, 5596 (1984).
[9]J. Budnick, J. Phys. (Paris) Colloq. **47**, C8-12 (1986).
[10]P. Boher *et al.*, J. Appl. Phys. **71**, 4 (1992).
[11]F. Baudelet *et al.* (unpublished).
[12]D. Raoux and M. DeSantis (private communication).
[13]M. Maurer *et al.*, Europhys. Lett. **9**, 803 (1989).
[14]G. Tourillon *et al.*, Phys. Lett. A **121** (1987).
[15]M. E. Kordesch and R. M. Hoffman, Phys. Rev. B. **29**, 491 (1984).
[16]D. E. Sayers, E. A. Stern, and F. W. Lytle, Phys. Rev. Lett. **27**, 1204 (1971).
[17]H. Magnan, thesis, University of Orsay (1990).
[18]J. Mimault *et al.*, J. Phys. F **11**, 1311 (1981).
[19](unpublished).
[20]M. Piecuch *et al.*, in *NATO Advanced Study Institute Series Proceedings,* edited by G. Hadjipanays (Plenum, New York, 1991), p. 195.
[21]L. M. Falicov *et al.*, J. Mater. Res. **5**, 1299 (1990).
[22]D. I. C. Pearson and J. M. Williams, J. Phys. F **9**, 1797 (1979).
[23]S. S. P. Parkin, N. More, and K. P. Roche, Phys. Rev. Lett. **64**, 2304 (1990).
[24]D. Knab and C. Koenig, J. Magn. Magn. Mater. **98**, 10 (1991).